Novel and Highly Recurrent Chromosomal Alterations in Sézary Syndrome

Maarten H. Vermeer,[1] Remco van Doorn,[1] Remco Dijkman,[1] Xin Mao,[3] Sean Whittaker,[3] Pieter C. van Voorst Vader,[4] Marie-Jeanne P. Gerritsen,[5] Marie-Louise Geerts,[6] Sylke Gellrich,[7] Ola Söderberg,[8] Karl-Johan Leuchowius,[8] Ulf Landegren,[8] Jacoba J. Out-Luiting,[1] Jeroen Knijnenburg,[2] Marije IJszenga,[2] Karoly Szuhai,[2] Rein Willemze,[1] and Cornelis P. Tensen[1]

Departments of [1]Dermatology and [2]Molecular Cell Biology, Leiden University Medical Center, Leiden, the Netherlands; [3]Department of Dermatology, St Thomas' Hospital, King's College, London, United Kingdom; [4]Department of Dermatology, University Medical Center Groningen, Groningen, the Netherlands; [5]Department of Dermatology, Radboud University Nijmegen Medical Center, Nijmegen, the Netherlands; [6]Department of Dermatology, Gent University Hospital, Gent, Belgium; [7]Department of Dermatology, Charite, Berlin, Germany; and [8]Department of Genetics and Pathology, Rudbeck Laboratory, University of Uppsala, Uppsala, Sweden

Abstract

This study was designed to identify highly recurrent genetic alterations typical of Sézary syndrome (Sz), an aggressive cutaneous T-cell lymphoma/leukemia, possibly revealing pathogenetic mechanisms and novel therapeutic targets. High-resolution array-based comparative genomic hybridization was done on malignant T cells from 20 patients. Expression levels of selected biologically relevant genes residing within loci with frequent copy number alteration were measured using quantitative PCR. Combined binary ratio labeling-fluorescence *in situ* hybridization karyotyping was done on malignant cells from five patients. Minimal common regions with copy number alteration occurring in at least 35% of patients harbored 15 bona fide oncogenes and 3 tumor suppressor genes. Based on the function of the identified oncogenes and tumor suppressor genes, at least three molecular mechanisms are relevant in the pathogenesis of Sz. First, gain of *cMYC* and loss of cMYC antagonists (*MXI1* and *MNT*) were observed in 75% and 40% to 55% of patients, respectively, which were frequently associated with deregulated gene expression. The presence of cMYC/MAX protein heterodimers in Sézary cells was confirmed using a proximity ligation assay. Second, a region containing *TP53* and genome maintenance genes (*RPA1/HIC1*) was lost in the majority of patients. Third, the interleukin 2 (IL-2) pathway was affected by gain of *STAT3/STAT5* and IL-2 (receptor) genes in 75% and 30%, respectively, and loss of *TCF8* and *DUSP5* in at least 45% of patients. In sum, the Sz genome is characterized by gross chromosomal instability with highly recurrent gains and losses. Prominent among deregulated genes are those encoding cMYC, cMYC-regulating proteins, mediators of MYC-induced apoptosis, and IL-2 signaling pathway components. [Cancer Res 2008; 68(8):2689–98]

Introduction

Sézary syndrome (Sz) is an aggressive type of cutaneous T-cell lymphoma/leukemia of skin-homing, $CD4^+$ memory T cells and is characterized by erythroderma, generalized lymphadenopathy, and the presence of neoplastic T cells (Sézary cells) in the skin, lymph nodes, and peripheral blood (1). Sz has a poor prognosis, with a disease-specific 5-year survival of ~24% (1).

Significant effort has been directed toward elucidating the molecular genetic events underlying this malignancy with the goal of facilitating early diagnosis and providing targets for directed therapeutic intervention. Cytogenetic and conventional comparative genomic hybridization (CGH) studies have uncovered a number of structural and numerical chromosomal aberrations in Sz, but highly recurrent genetic lesions have not been identified (2–7). Gene expression profiling of Sézary cells has revealed deregulated expression of several oncogenes and tumor suppressor genes, including *TGF-β receptor II, JUNB, STAT4, MMP9, MXI1,* and *TWIST* (8–11).

Although many genetic alterations have been identified in previous studies, the small number of included patient samples and variation of the criteria used for the diagnosis of Sz have resulted in differing results and has impeded the delineation of genetic alterations typical of this malignancy. In addition, the low resolution of the cytogenetic analyses applied has limited the identification of presumed Sz-relevant genes located in regions with chromosomal alteration. In this multicenter study, we aimed to obtain a detailed catalogue of numerical and structural chromosomal abnormalities in a large group of well-defined Sz patients using high-resolution array-based CGH in combination with combined binary ratio labeling (COBRA), fluorescence *in situ* hybridization (FISH), and *in situ* proximity ligation assays (PLA).

Materials and Methods

Selection of patients. Cryopreserved or fresh blood samples from 20 patients with Sz (10 males, 10 females; median age, 69 y) were available for inclusion in this study (clinical characteristics are summarized in Supplementary Table S1). Diagnosis of Sz was based on criteria defined in the WHO/European Organization for Research and Treatment of Cancer classification (1). All patients presented with erythroderma and showed highly elevated CD4/CD8 ratios and clonality of T cells in peripheral blood. Follow-up data revealed that nine patients had died of Sz; the median survival time was 31 mo. In all patients, peripheral blood mononuclear cells (PBMC) were isolated by Ficoll density centrifugation. From patients 3, 4, 5,

Note: Supplementary data for this article are available at Cancer Research Online (http://cancerres.aacrjournals.org/).

Requests for reprints: Cornelis P. Tensen, Department of Dermatology, T02-03, Leiden University Medical Center, P.O. Box 9600, 2300 RC Leiden, the Netherlands. Phone: 31-71-526-9369; Fax: 31-71-524-8106; E-mail: c.p.tensen@lumc.nl.

doi:10.1158/0008-5472.CAN-07-6398

and 7, $CD4^+$ T cells were subsequently isolated from PBMCs by negative selection with magnetic beads ($CD4^+$ T-cell isolation kit, Miltenyi Biotec).

$CD4^+$ T cells isolated with MACS beads from peripheral blood of three patients with an erythroderma secondary to atopic dermatitis and seven healthy donors (of which six were *in vitro* activated as previously described; ref. 12) were used as controls for quantitative PCR experiments.

Approval for these studies was obtained from the respective institutional review boards. Informed consent was provided according to the Declaration of Helsinki.

Extraction of DNA and RNA. DNA was isolated from 1×10^7 Ficoll purified lymphocytes with the Genomic-tips 20/G kit (Qiagen). RNA was extracted from isolated $CD4^+$ T cells (Sz patients or controls) with the RNeasy kit (Qiagen).

Array-based CGH and data analysis. Genome-wide analysis of DNA copy number changes of patient samples was done with high-resolution array-based CGH. Fabrication and validation of the array, hybridization methods, and analytic procedures have been described elsewhere in detail (13, 14). The particular bacterial artificial chromosome (BAC) set used to produce these arrays is distributed to academic institutions by the Wellcome Trust Sanger Institute (Cambridge, United Kingdom) and contains 3,500 individual BACs each harboring ≈100 kb targets spaced at ≈1 Mb density, thus covering 10% of the full genome. Genomic positions were established based on National Center for Biotechnology Information Build 35, Ensembl database version 36.35. Data were analyzed using CAPWeb and visualized using VAMP (15). Candidate genes were selected from the "Atlas of Genetics and Cytogenetics in Oncology and Haematology,"[9] whereas bona fide oncogenes and tumor suppressor genes within this list were identified using the Cancer Gene Census list.[10]

Several seemingly isolated gains and losses involving single reporter BAC clones only (e.g., 5p15.33, 1p21.1) were excluded from the analysis because they reside in regions with described copy number variations.[11]

Quantitative real-time PCR. cDNA synthesis was done on 1 μg of total RNA after treatment with RQ1 DNase I (Promega), using IScript reverse transcriptase (Bio-Rad), oligo(dT)12–18, and random hexamere priming (Bio-Rad) in a final volume of 20 μL. Real-time PCR was done with the MyIQ instrument and the SYBR Green Supermix (Bio-Rad). Primer sequences (oligos synthesized by Invitrogen and developed using Beacon Designer, Bio-Rad) for amplification of selected transcripts are given in Supplementary Table S2.

The cycle parameters for transcripts of interest and for the reference gene *RPS11* used for normalization were as follows: denaturation for 15 s at 95°C; annealing and extension for 20 s at 60°C, for 40 cycles. Data were evaluated using the MyIQ software (Bio-Rad) and the second derivative maximum algorithm, whereas confirmation of the specificity of the PCR product and standard curves were done as previously described (16).

COBRA-FISH. COBRA-FISH analysis was done on short-term cultures of peripheral blood samples from five patients (numbers 2, 3, 5, 6, and 7 in Supplementary Table S1). In all samples, chromosome condensation was chemically induced and resulting chromosome preparations were hybridized according to previously described protocols (17, 18).

***In situ* PLA.** MACS-isolated $CD4^+$ Sézary cells (patient 1, 3, and 7) or control $CD4^+$ T cells from a healthy control were either stimulated [phytohemagglutinin (PHA) 1 μg/mL and interleukin 2 (IL-2) 100 units/mL and harvested after 2, 8, and 24 h] or deposited directly on glass slides using a cytospin centrifuge. Cytospins were stained for cMYC/MAX heterodimers by *in situ* PLA, and the number of *in situ* PLA signals per cell was counted by semiautomated image analysis using the freeware software BlobFinder[12] as previously described (19, 20). We used an epifluorescence microscope (Axioplan II, Zeiss), equipped with a 100-W mercury lamp, a charge-coupled device camera (C4742-95, Hamamatsu), and a computer-controlled filter wheel with excitation and emission filters for visualization of 4′,6-diamidino-2-phenylindole, FITC, Cy3, and Cy5. We used a 63× objective (Plan-Neofluar, Zeiss) for all images. We collected images using the AxioVision LE 4.3 software (Zeiss) and thresholded them using Adobe Photoshop CS (Adobe Systems). The *in situ* PLA method has been developed to examine the subcellular localization of protein-protein interactions at single molecule resolution. Proximity probes (oligonucleotides attached to antibodies against the two target proteins) guide the formation of circular DNA strands when bound in close proximity. The DNA circles in turn served as templates for localized rolling-circle amplification, allowing individual interacting pairs of protein molecules to be visualized and counted.

Results

Chromosomal gains are more frequent than losses in Sézary syndrome. In all 20 Sz patients, multiple chromosomal imbalances were identified. Overall, gains were more frequent than losses. A ratio plot of a single Sz patient (number 2 in Table S1), an cumulative dot plot/heatmap of all data, and a corresponding frequency plot of gains and losses for all Sz samples are shown in Fig. 1*A* to *C*. These data were used by VAMP to demarcate recurrent minimal genomic alterations (15, 21) in tumor cells using a threshold of 35% and excluding the X and Y chromosomes (Fig. 1*D*; Table 1).

Two broad regions and several focal areas of gains were frequently observed in Sz samples. Most involved was the long arm of chromosome 17 with a complex pattern. In at least 80% of the patients, gains were observed in the region 17q21.31–17q23. Gains at 8q24.1–q24.3 were detected in 15 of 20 (75%) samples; 5 minimal common regions of gain at chromosome 8 could be distinguished at megabase positions 42.15–42.67, 50.88–58.10, 62.41–79.80, 101.25–113.66, 127.56–136.65, and 139.31–146.17. Using the frequency of amplifications, gains and losses (FrAGL) option of VAMP, highly recurrent isolated gains were found at 2p11.2, 4p16.1, and 7p21.1.

The most frequent regions of loss were found at chromosomes 17 and 10 and (albeit to a lesser extent) at chromosomes 2, 5, 12, and 13. The most frequently lost region consisted of 17p13 to 17p12 detected in 15 of 20 (75%) samples, with a peak at 17p13.1–17p11.2 (Mb 6.07–7.68). Multiple discrete minimal overlapping regions of loss could be identified at chromosome 10: one at the short arm [10p11.22 (Mb 29.84–33.17)] and seven at the long arm of the chromosome in the region from 10q22–10q26 (see Table 1). In addition, highly recurrent isolated losses were observed at 3q26.33, 5q14.3, 7p14.1, 9p13.1–9p12, and 16p11.2.

COBRA-FISH. In five patients, COBRA-FISH was done to analyze structural chromosomal alterations. This detailed karyotyping complements the array-CGH data by detecting polyploidy (e.g., 3n or 4n) and balanced rearrangements (translocation, inversion). As in previous studies (2, 3), several structural rearrangements were observed in all five cases, but no recurrent translocation breakpoints were identified (example given in Supplementary Fig. S1; results summarized in Supplementary Table S3). The most frequently observed alterations involved chromosomes 10 and 17, detected in all five cases; chromosome 8, detected in four of five cases; and chromosome 12, detected in three of five cases. Recurrent interstitial deletion of chromosome 10q24 region was observed in three of five patients, confirming array-CGH results.

Candidate genes residing in loci with copy number alteration. Copy number alterations may have a causative role in oncogenesis

[9] http://atlasgeneticsoncology.org/
[10] http://www.sanger.ac.uk/genetics/CGP/Census/chromosome.shtml
[11] http://projects.tcag.ca/variation/
[12] http://www.cb.uu.se/~amin/BlobFinder/

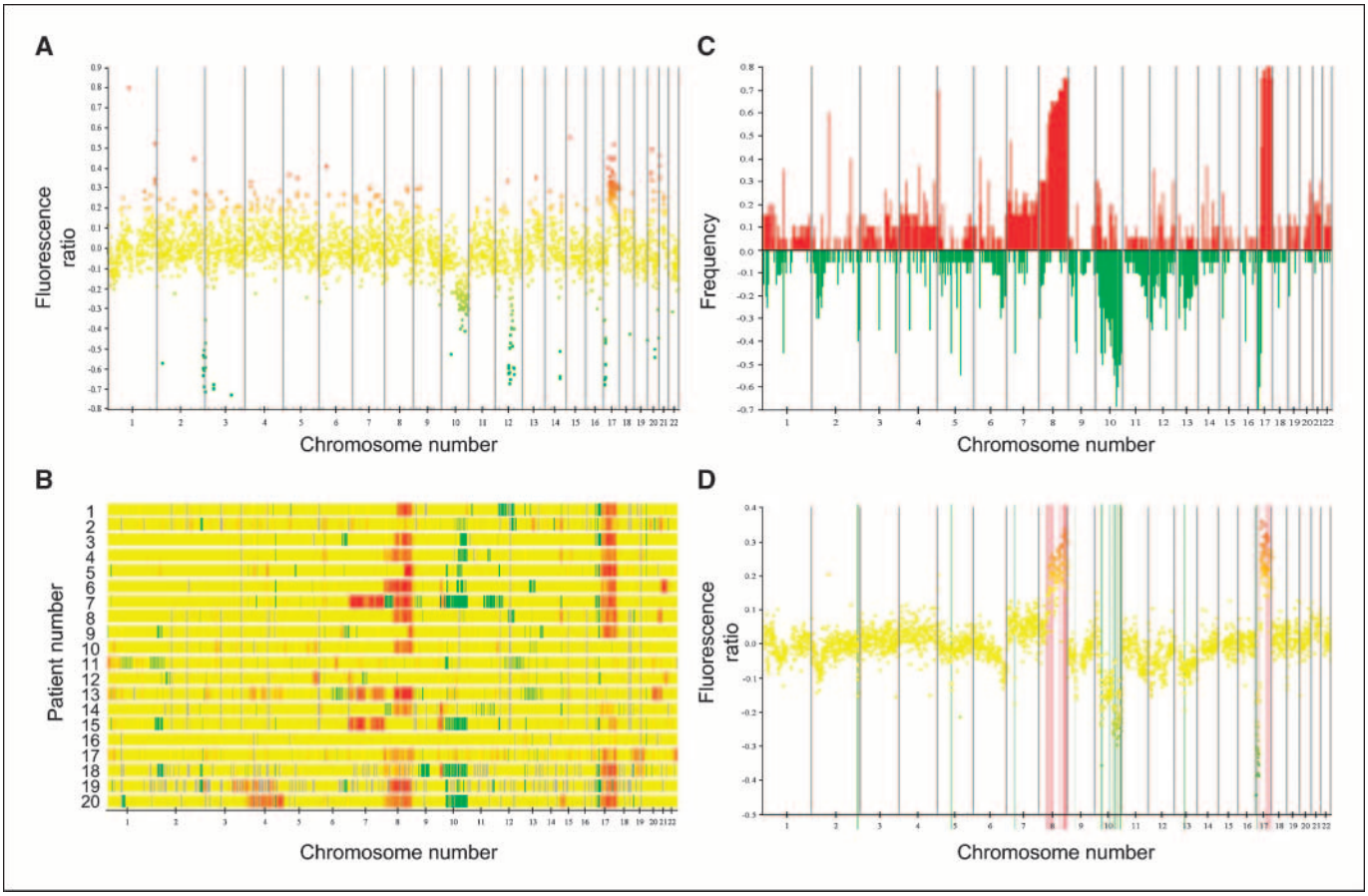

Figure 1. VAMP output of array-CGH data. All data are presented ordered by chromosomal map position of the clones (excluding X and Y chromosomes). *A,* VAMP analysis of array-CGH data obtained from a single patient (number 2 in supplementary Table S1). Gains are in red, losses in green, and absence of alterations in yellow. Respective chromosomes are indicated with a number, and chromosome boundaries with vertical lines. *B,* dot plot depicting the results of all 20 patients, with color coding as in *A*; chromosome boundaries are omitted for clarity. *C,* overall frequency of DNA copy number alterations (*CNA*) in Sz calculated using the FrAGL option of VAMP. Lower columns (*green*) represent losses and the upper columns (*red*) represent gains. *D,* averaged CGH data of all 20 patients and minimal common regions of loss (*green*) and gain (*red*) as calculated by VAMP (threshold, 35%).

through deregulation of the expression of genes residing in the affected chromosomal region. Using the high-definition picture of the Sz genome as summarized in Table 1, we examined minimal common regions in more detail. We screened the data for consistency of recurrences of particular genes and identified 15 bona fide oncogenes and 3 tumor suppressor genes, as well as genes involved in cytokine signaling and in the control of integrity of the genome in the affected loci (Supplementary Table S4).

Oncogenes and tumor suppressor genes. The bona fide oncogene most frequently affected by gain in the Sz genome was the *cMYC* oncogene (15 of 20 cases, 75%) on chromosome 8. Moreover, we found losses of the cMYC regulating genes *MXI1* (on chromosome 10q25) and *MNT* (on chromosome 17p13) in at least 8 and 11 cases, respectively. Gain of *cMYC* was accompanied by loss of *MXI1* in at least 7 of 20 patients, loss of *MNT* in 9 of 20 patients, and a combination of *MXI1* and *MNT* loss in 6 of 20 patients. Isolated loss of *MXI1* or *MNT* was found in one patient. In aggregate, 18 of 20 patients had defects in *cMYC* and/or *cMYC* antagonists.

To protect cells from the oncogenic potential of continuous cMYC activity, cMYC protein promotes apoptosis by induction of BIM leading to the release of cytochrome *c* from mitochondria and through the p14ARF-Mdm2-TP53 pathway (22, 23), which is controlled by TWIST (24, 25). We detected loss of 17p13.2 harboring *TP53* and loss of 2q12, leading to loss of *BIM* in 15 of 20 and 1 of 20 patients, respectively. There was gain of a chromosomal region on 7p21 containing the *TWIST* gene in at least 1 but potentially 8 of 20 (40%) patients. Loss of 9p21, affecting *CDKN2A* (encoding p14ARF and p16), was detected in 3 patients. Combined, recurrent genetic lesions in *TP53, BIM, TWIST,* or *CDKN2A* that may contribute to abrogation of the cMYC-induced apoptotic response was observed in 16 of 20 (80%) of patients.

Finally, we noticed loss of the tumor suppressor gene FAS (on chromosome 10q24), a key regulator of apoptosis in mature T cells (26), in nearly half of the Sz patients.

Aberrations in genes affecting cytokine signaling. T-cell activation and proliferation is critically dependent on autocrine/paracrine stimulation through the IL-2 receptor (IL-2R). We identified gains of regions harboring the *IL-2, IL-2Rα,* or *IL-2Rβ* genes in 10% to 30% of Sz patients. Gain of both *IL-2Rα* and *IL-2Rβ* or gain of one of the receptor chains and the *IL-2* gene was encountered in three patients. In addition, deletion of *TCF8* (also known as *ZEB1*), a gene encoding a zinc finger transcription factor that represses IL-2 expression in T cells, was detected in at least 9 of 20 (45%) of the patients. In seven patients, gain of IL-2R components was accompanied by deletion

Table 1. Minimal recurrent chromosomal aberrations in Sézary syndrome

Cytogenetic band	Adjacent clones		Mb		Size	Candidate genes	Sézary syndrome (n = 20)
	Start	Stop	Start	Stop			Total (%)
Gain and amplification							
2p11.2*	RP11-495B16	RP11-513O19	82.61	85.57	2.94	*TMSB10, KCMF1, TCF7L1, CAPG*	60
4p16.1*	RP11-338K13	RP11-61G19	8.00	10.21	2.21	*HTRA3, ACOX3*	40
7p21.1*	RP11-403N12	RP11-71F18	16.67	19.21	2.44	*TSPAN13, AGR2, AGR3, AHR, HDAC9,* ***TWIST1***	40
8p11.2–8p11.1	RP11-231D20	RP11-503E24	41.52	43.32	1.80	*ANK1, MYST3, PLAT, IKBKB, POLB, SLC20A2, THAP1, FNTA, FLJ23356*	40
8q11.2–8q12	RP11-401N18	RP11-342K10	49.94	58.23	8.29	*SNAI2, SNTG1ST18, RB1CC1, RGS20, TCEA1, LYN, MOS, PLAG1, PENK, CYP7A1, SDCBP, NSMAF, TOX*	60
8q12–8q21.1	RP11-227F6	RP11-523D2	61.92	80.73	18.81	*ASPH, GGH, CYP7B1, DNAJC5B, TRIM55, CRH, ADHFE1, MYBL1, PTTG3, COPS5, ARFGEF1, CPA6, DEPDC2, SULF, NCOA2, TRAM1, TERF1, TCEB1, ZFHX4,* ***IL-7***	65
8q22–8q23	RP11-10G10	RP11-11A18	99.22	115.76	16.54	*HRSP12, STK3, COX6C, FBXO43, RNF19, PABPC1, RRM2B, EDD1, KLF10, ATP6, V1C1, BAALC, FZD6, CTHRC1, WDSOF1, RIMS2, DPYS, LRP12, ZFPM2, ABRA, ANGPT1, RSPO2, EIF3S6, TMEM74, NUDCD1, EBAG9,*	70
8q24.1–8q24.2	RP11-28I2	RP11-343P9	126.80	137.77	10.98	*FAM84B,* ***MYC,*** *PVT1, MLZE, DDEF1, ADCY8, OC90, HHLA1, KCNQ3, TG, WISP1, NDRG1, KHDRBS3*	75
8q24.2–8q24.3	RP11-172M18	RP5-1056B24	137.79	146.00	8.21	*KCNK9, NIBP, C8orf17, PTK2, PTP4A3, BAI1, PSCA, C8orf55, SLURP1, LYNX1, GML, LY6E, GLI4, MAFA, EEF1D, SCRIB, NRBP2, GPAA1, CYC1, BOP1, HSF1, SCRT1, ADCK5, VPS28, FOXH1, PPP1R16A, RECQL4, LRRC14*	75
17p11.2	RP1-162E17	RP11-78O7	17.94	20.01	2.07	*SPECC1, USP22, MAP2K3, KCNJ12*	45
17q21.31	RP11-156E6	RP11-948G15	37.19	38.43	1.24	***STAT5A/STAT5B/STAT3***	70
17q23	RP11-506H21	RP11-332H18	52.62	57.30	4.68	*MSI2, MPO, SUPT4H1, RNF43, 38231, TEX14, RAD51C, PPM1E, TRIM37, DHX40, CLTC, RPS6KB1, ABC1, APPBP2, PPM1D, BCAS3, TBX2, BRIP1, INTS2*	80
17q23	RP11-156L14	RP11-156L14	57.87	59.63	1.75	*TLK2, CYB561, ACE, MAP3K3, LYK5, DDX42, SMARCD2, GH2, GH1, CD79B, ICAM2, ERN1*	85
17q24–17q25	RP11-166M16	RP11-387C17	66.19	69.45	3.25	*SOX9, SSTR2, C17orf80, TTYH2*	80
17q25	RP11-398J5	GS-362-K4	73.64	81.50	7.86	*TMC6, TMC8, TK1, BIRC5, EPR1, SOCS3, PSCD1, TIMP2, LGALS3BP, C1QTNF1, ENPP7, CBX8, CBX4, EIF4A3, CARD14, KIAA1618, FLJ35220, AATK, ACTG1, HGS, SIRT7, MAFG, ASPSCR1, STRA13, GPS1, FASN, CSNK1D, CD7, FOXK2, RAB40B, FN3KRP, FN3K*	70
Loss and deletion							
2q37	RP11-419H23	RP11-91N19	231.79	232.99	1.20	*NCL, PTMA, COPS7B, ALPPL2,*	40
3q26.33*	RP11-682A21	RP11-534H15	180.29	181.44	1.15	*PIC3CA, GNB4*	45
5q13	RP11-421A17	RP11-115I6	67.68	71.66	3.98	*PIK3R1, CCNB1, CENPH, CDK7, TAF9, RAD17, OCLN, NAIP, GTF2H2, MAP1B*	45
5q14.3*	RP11-3B10	RP11-349M12	112.16	115.97	3.81	*ZRSR1, MCC, TRIM36, PGGT1B*	55
7p14	RP11-121A8	RP11-273L18	37.60	39.28	1.68	*SFRP4, EPDR1, TRGA, TRGV9, AMPH, POU6F2*	45
9p13.1–9p12	RP11-395E19	RP11-268E1	40.77	44.51	3.74	**No annotated cancer related genes**	45
10p11.2	RP11-14C22	RP11-472N13	29.84	33.17	3.33	*BAMBI, TCF8, MAP3K8, ZEB1, ARHGAP12, KIF5B, EPC1,*	40
10q22	RP11-326F3	RP11-345K20	72.65	75.73	3.08	*PRF1, ADAMTS14, SGPL1, UNC5B, PSAP, ASCC1, DDIT4, DNAJB12, P4HA1, DNAJC9, ANXA7, PPP3CB, CAMK2G*	40

(*Continued on the following page*)

Table 1. Minimal recurrent chromosomal aberrations in Sézary syndrome (Cont'd)

Cytogenetic band	Adjacent clones		Mb		Size	Candidate genes	Sézary syndrome (n = 20)
	Start	Stop	Start	Stop			Total (%)
10q23.31	RP11-399O19	RP11-15K3	90.44	92.92	2.49	*ACTA2,* ***FAS***	50
10q23.32	RP11-430L14	RP11-162K11	93.74	95.77	2.04	*BTAF1, MARCH5, IDE, KIF11, HHEX, FER1L3, LGI1, PLCE1*	50
10q24–10q25	RP11-264H19	RP11-373N18	103.28	105.83	2.55	*TLX1, BTRC, POLL, FGF8, MGEA5, LDB1, NFKB2, PSD, ACTR1A, SUFU, TRIM8, ARL3, CYP17A1, NT5C2, PCGF6, PDCD11, NEURL, SH3PXD2A, SLK, COL17A1*	60
10q25.2	RP11-163F15	RP11-381K7	110.24	112.96	2.73	*ADD3,* ***MXI1, DUSP5,*** *SMC3, PDCD4,*	60
10q25–10q26	RP11-5G18	RP11-62L18	118.69	123.21	5.42	*GFRA1, HSPA12A, EMX2, CASC2, PRLHR, NANOS1, EIF3S10, PRDX3, RGS10, TIAL1, BAG3, INPP5F, BRWD2, FGFR2*	50
10q26	RP11-115N19	RP11-400F15	126.61	131.82	5.21	*ZRANB1, CTBP2, MMP21, BCCIP, DHX32, ADAM12, DOCK1, PTPRE, MKI67, MGMT*	45
13q14	RP11-185C18	RP11-327P2	49.07	51.24	3.35	*RCBTB2, PHF11, RCBTB1, ARL11, KPNA3, TRIM13, KCNRG, DLEU2, DLEU1, FAM10A4, DLEU7, RNASEH2B, INTS6*	35
16p11.2*	RP11-388M20	RP11-374A17	31.19	33.54	2.35	*ITGAM, ITGAX, ITGAD, COX6A2, TGFB1I1, SLC5A2, TP53TG3*	40
17p13.3–13.1	RP11-216P6	RP11-135N5	1.01	2.32	1.31	*PRPF8, SERPINF1, SMYD4,* ***RPA1,*** *DPH1, OVCA2,* ***HIC1, MNT,***	55
17p13.1	RP11-243K12	RP11-404G1	5.92	7.71	1.69	*AIPL1, PITPNM3, TXNL5, XAF1, ALOX12, BCL6B, CLEC10A, GABARAP, CLDN7, SLC2A4, YBX2, EIF5A, KCTD11, TNK1, FGF11, POLR2A, TNFSF12, TNFSF13, EIF4A1, CD68, FXR2, SHBG, ATP1B2,* ***TP53,*** *EFNB3, JMJD3, CHD3*	75
17p12	RP11-208F13	RP11-385D13	9.47	15.32	6.85	*RCVRN, GAS7, SCO1, MAP2K4, ELAC2, COX10*	70

*Denotes aberrations identified by FrAGL (threshold, >35%); other aberrations are identified using the minimal common region option of VAMP (threshold, 35%). Genes discussed in the text are in bold; oncogenes and tumor suppressor genes are underlined.

of *TCF8*. Taken together, in 13 of 20 (65%) of Sz patients, genetic alterations potentially leading to increased IL-2 signaling were found.

Gain of the *STAT3* and *STAT5A/STAT5B* genes, the major transducers of the IL-2 cytokine signaling pathway that are localized as a tandem on the genome, was detected in 15 of 20 (75%) of Sz patients. Finally, loss of DUSP5, an inhibitor of IL-2 signaling (27), was found in 11 of 20 (55%) of patients. Combined, gains of STAT3/STAT5 and/or loss of DUSP5 was found in 17 of 20 (85%) patients.

In addition to gain of IL-2 signaling components, we also observed gain of a chromosomal region encoding the *IL-7* gene (8q12–8q21.1) in 65% of the cases.

Genetic instability. This study as well as previous cytogenetic studies shows that the Sz genome harbors numerous chromosomal abnormalities, indicating that chromosomal instability is an important characteristic of this malignancy. We therefore focused on genes present in minimal common regions, loss of which may contribute to genetic instability. In 11 of 20 (55%) Sz patients, a loss of 17p13.3–13.1 on the short arm of chromosome 17 was detected. This region harbors at least two candidate tumor suppressor genes involved in genome maintenance: hypermethylated in cancer 1 (*HIC1*) and replication protein 1 (*RPA1;* refs. 28, 29).

Confirmation of alterations in gene expression by quantitative real-time PCR. For eight Sz patients, the expression of cMYC, MNT, MXI1, and TWIST (all belonging to the cMYC network) was compared with $CD4^+$ T cells isolated from peripheral blood of patients with erythroderma secondary to atopic dermatitis (n = 3) and normal naïve (n = 1) and *in vitro* activated $CD4^+$ T cells from healthy controls (n = 6; Fig. 2).

In seven of eight Sz patients, cMYC levels were higher when compared with naïve or *in vitro* activated $CD4^+$ T cells, whereas in $CD4^+$ T cells from erythrodermic atopic dermatitis patients, comparable to slightly higher cMYC levels were found (Fig. 2). Expression of TWIST was only detected in Sz patients and was observed in seven of eight Sz patients tested. MNT and MXI were expressed at low levels in six and eight Sz patients, respectively. In benign controls, higher expression for MXI1 was observed in two patients with atopic dermatitis, and higher expression for MNT was found in three atopic dermatitis patients as well as two samples of activated T cells.

Detection of cMYC expression and heterodimerization with MAX using *in situ* PLA. Expression of cMYC protein and heterodimerization with its obligatory partner MAX were visualized by *in situ* PLA (Fig. 3). Quantification of the number of *in situ* PLA signals per cell revealed significantly higher expression of cMYC/MAX heterodimers in three Sz patients (Sz patients 1, 3,

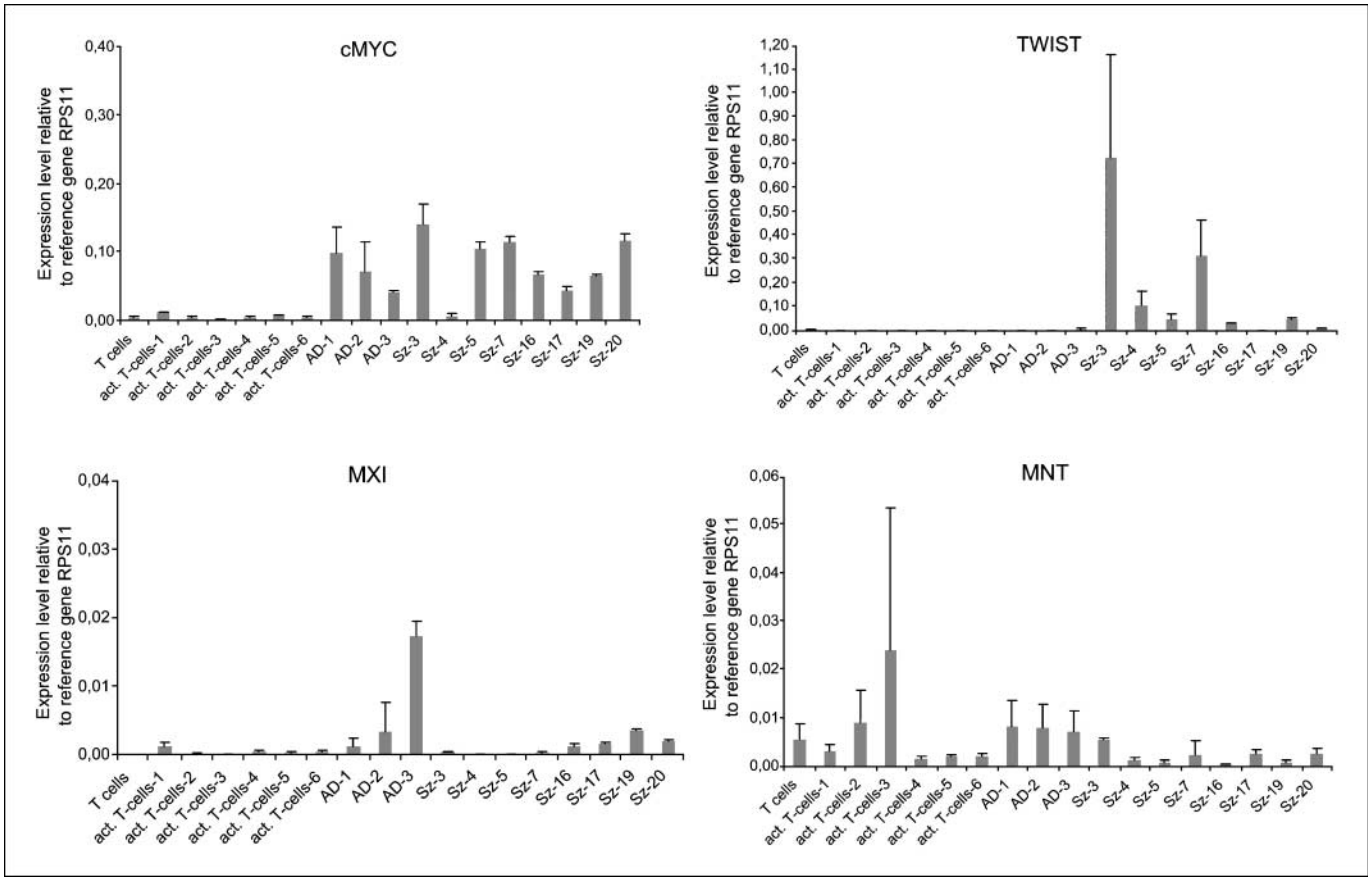

Figure 2. mRNA expression in Sz samples and controls as measured by quantitative real-time PCR. *Columns,* mean of three independent quantitative real-time PCR experiments, depicted relative to the reference gene *RPS11*; *bars,* SE.

and 7) compared with controls ($CD4^+$ T cells). In addition, in a time course experiment done with Sz cells from patient 7, we observed increased expression of cMYC/MAX heterodimers in Sz cells 2, 8, and 24 hours after stimulation with PHA and IL-2 compared with $CD4^+$ T cells.

Discussion

To identify genetic events underlying the pathogenesis of Sz, we conducted a high-resolution analysis of recurrent copy number alterations and structural chromosomal abnormalities in tumor cells from 20 patients diagnosed with Sz according to the criteria of the WHO-European Organization for Research and Treatment of Cancer classification (1).

Our array-CGH method provides improved mapping resolution over previously reported cytogenetic studies and permitted the identification of candidate genes contributing to the pathogenesis of Sz. In addition to fine-mapping of previously described chromosomal alterations, we identified several novel recurrent genetic lesions. Using COBRA-FISH, we detected unbalanced translocations affecting 17p10 ~ p11 and 6q22 ~ 23 in four of five and two of five patients with deletion of the proximal or distal regions, respectively.

The chromosomal regions showing gain most frequently include 17q23–17q25 and 8q24.1–8q24.3. Chromosomal loss was detected most frequently at 17p13.1 and 10q25. Previous cytogenetic and allelotyping studies in Sz identified 10q22–26 as the chromosomal region most frequently affected by both deletions and unbalanced translocations (2, 4). The present study enabled identification of eight discrete regions of highly recurrent loss in chromosome 10: a novel one at the short arm (10p11.22) and seven at the long arm between 10q22 and 10q26. The deletions at 10q23.32 and 10q24–10q25.1 were described before in a fine-mapping allelotyping study (30). The other losses represent novel genetic lesions in Sz. Of interest, the loss at 10q23.31 contains the *FAS* gene, and the loss on 10q25.1–10q25.2 includes the *MXI1* and *DUSP5* genes. The region on 10p11.22 harbors the *TCF8* gene.

A recent publication indicated that deletions or translocations affecting the *NAV3* gene encoded at 12q21 are found in most Sz patients (9). In the present study, we identified deletions in this region in a minority of patients (at most 6 of 20, 30%; see Supplementary Table S4). We recognized a previously described deletion in the 6q22–24 region (3) in a minority of our patients (25%); according to our analysis, it encompasses a 14.35-Mb fragment between Mb 137.13 and 151.49.

Taking advantage of the high resolution of our analysis, we sought to identify genes, deregulation of which may contribute to the development or progression of Sz. First, we focused on oncogenes and tumor suppressor genes, including *cMYC* family genes and *TP53*, residing in minimal common regions within highly recurrent copy number alteration. Given the central role of the IL-2 pathway in the proliferation of mature T cells from which Sz cells are derived, we additionally examined copy number alteration and expression of genes encoding components of this pathway.

cMYC family proteins, cMYC antagonists, and cMYC-induced apoptosis. In the present study, we identified increased expression and gain of chromosomal regions harboring cMYC and loss and decreased gene expression levels of the cMYC antagonists MXI1 and/or MNT in the large majority of Sz patients. This is in accordance with previous gene expression studies by our group reporting low expression of MXI1 and MNT in Sz cells (11). Deregulated expression of cMYC has been implicated in the etiology of a wide range of hematologic malignancies (31, 32). Increased amounts of the oncogenic transcription factor cMYC contribute to tumorigenesis by promoting proliferation, inhibiting differentiation, and increasing genomic instability (33, 34). The cMYC protein requires heterodimerization with MAX to function as a transcription factor. MNT and MXI1 also interact with MAX thereby acting as transcriptional repressors of cMYC. Consistent with the proposed cMYC antagonist function, recent studies showed that in mice loss of Mnt and Mxi1 can promote proliferation and facilitate tumorigenesis, leading to disrupted T-cell development and ultimately T-cell lymphomas (35, 36). In Sz cells, gene expression levels of cMYC were comparable to $CD4^+$ T cells from erythrodermic atopic dermatitis patients, which are known to be highly activated, proliferating T cells. However, in contrast to samples from Sz patients, the atopic dermatitis samples also

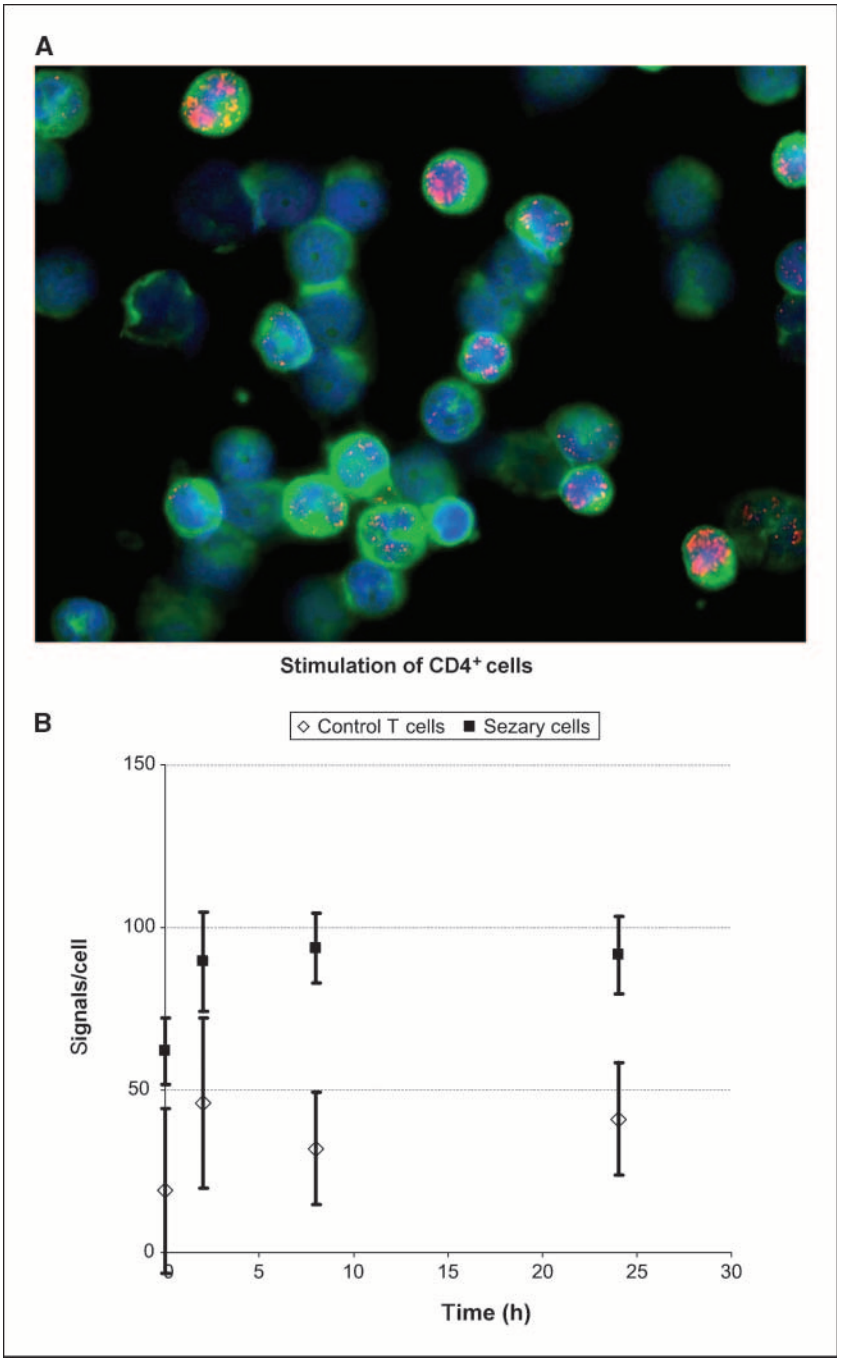

Figure 3. Detection of endogenous cMYC/MAX heterodimers in Sézary cells by *in situ* PLA. *A,* cytospin of $CD4^+$ T cells from Sz patient 3. cMYC/MAX heterodimers were visualized by staining cells with proximity probes directed against cMYC and MAX, followed by ligation and amplification as outlined in ref. 22. The hybridization probes were labeled with Alexa 555 (*red*), the cytoplasm was counterstained with FITC-labeled antibody to actin (*green*), and the nuclei were stained with Hoechst 33342 (*blue*). *B,* quantification of signals and comparison with a healthy donor. MACS-isolated $CD4^+$ T cells from a Sézary patient (Sz 7) or from a healthy control were stimulated with PHA 1 μg/mL and IL-2 100 units/mL and samples were drawn at 0, 2, 8, and 24 h after stimulation. Signals were quantified as described (23).

expressed MNT and, to a lesser extent, MXI1, in line with intact physiologic regulatory control of cMYC expression (35–37). In line with the hypothesized deregulation of cMYC in Sz, we detected increased expression of cMYC/MAX heterodimers in Sz cells compared with controls, suggesting that the increased levels of cMYC mRNA are associated with increased transcriptional activity.

cMYC-induced apoptosis acts as a threshold to malignant transformation, and additional genetic alterations that hamper cMYC-induced apoptosis through disruption of downstream effector molecules or by specific mutations in cMYC can profoundly accelerate cMYC-dependent tumor progression. Mutations of TP53 or p14ARF collaborate with cMYC in the induction of lymphomas (23), whereas high expression of TWIST can inhibit the proapoptotic effect of cMYC through inhibition of the p14 ARF/TP53 pathway in neuroblastoma (24). The present study suggests that in Sz, this cMYC feedback system is abrogated by deletions of 17p13.2, leading to loss of TP53, deletions of 9p21 containing *CDKN2A,* which encodes p14ARF, as well as gain of a region in 7p21 containing the *TWIST* gene. These observations are in line with previous studies showing that TWIST is highly expressed in Sz cells compared with non-malignant $CD4^+$ T cells (11).

Taken together, 18 of 20 Sz patients harbored genetic lesions potentially leading to increased levels of cMYC that were accompanied by defects in the cMYC-induced apoptosis in 16 of 20 patients, thus strongly suggesting that deregulation of the cMYC signaling network is a pivotal event in the pathogenesis of Sz.

Cytokine and STAT signaling. Recent studies have led to the recognition that autocrine/paracrine signaling of IL-2, IL-7, and IL-15 cytokines, resulting in phosphorylation of STAT3 and STAT5 proteins, plays a crucial role in the pathogenesis of Sz (38–41). Our array-CGH results provide a rationale for the activation of this cytokine signaling pathway because gain of *IL-2, IL-2Rα,* and *IL-2Rβ,* combined with gain of the STAT3/STAT5 cluster and deletions of *DUSP5* and *TCF8,* which inhibit IL-2 production and IL-2 signaling, respectively (27, 42), was shown in the majority of patients. Deregulated stimulation through the IL-2R combined with disrupted apoptosis (e.g., by loss of the *FAS* gene, which was detected in at least 45% of the patients) is likely to be responsible for uncontrolled proliferation. Gain of chromosomal DNA encoding the *IL-7* gene in 65% of the patients suggests that the observed elevated IL-7 protein levels in cutaneous T-cell lymphoma patients might not only result from production by skin cells (43) but could, in part, also be the result of secretion by tumor cells themselves as was previously postulated (44).

Chromosomal instability and epigenetic modifications. Focal deletions at 17p13.3–17p13.1 leading to loss of *TP53, RPA1,* and *HIC1* was detected in the majority of Sz patients and may play an important role in the widespread chromosomal and genetic instability that is a characteristic feature of this disease. Loss of HIC1 function promotes tumorigenesis by loss of direct transcriptional repression of SIRT1, leading to deacetylation of TP53, whereas loss of RPA1 directly impairs DNA double-strand break repair and maintenance of chromosomal stability (28, 29). The synergy between Hic1 and Tp53 in tumor suppression is illustrated by studies in knockout mice showing that germ-line disruption of one copy each of HIC1 and TP53 on opposite chromosomes (trans) or on the same chromosome (cis) resulted in an altered spectrum, earlier appearance, increased prevalence, and aggressiveness of tumors (45).

Recent experiments in mice showed that Rpa1 function is essential for DNA double-strand break repair maintenance of chromosomal stability and tumor suppression. Mice carrying a heterozygous missense change in one of the DNA-binding domains of Rpa1 developed lymphoid tumors characterized by large-scale chromosomal changes as well as segmental gains and losses (46). Combined, the loss of TP53, HIC1, and RPA1 in Sézary cells will probably contribute to genetic instability.

Hypothetical model of the pathogenesis of Sézary syndrome. Collectively, the results of this study show that the Sz genome is characterized by a combination of highly recurrent chromosomal alterations. Prominent among genes residing in minimal common regions are genes encoding cMYC, cMYC-regulating proteins, and mediators of cMYC-induced apoptosis. In

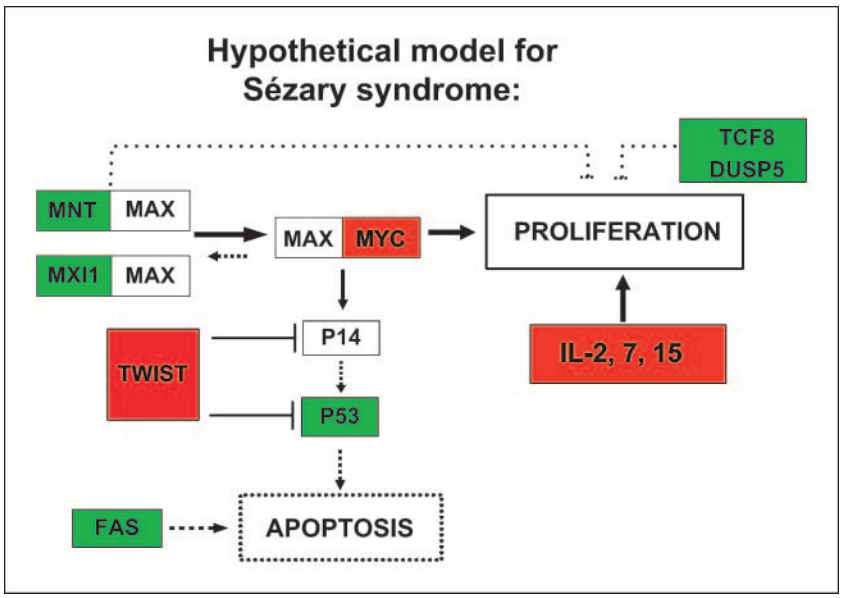

Figure 4. A hypothetical model describing oncogenic and aberrant proliferative events in Sézary cells. *Red,* amplified genes; *green,* deleted genes. *Filled lines,* putative enhanced activity resulting from gain; *dotted lines,* putative decreased activity as a result of loss. *Arrows,* stimulatory effects; *ended lines,* inhibitory functions.

addition, these loci harbor IL-2 signaling pathway component genes known to encode critical regulators of T-cell proliferation and genes involved in the maintenance of genetic stability. Whether these specific chromosomal alterations occur at the first steps of tumor development or are selected for during progression of the disease is at present unknown. Hypothetically, the combined signaling alterations that may occur as a consequence of the observed genetic alterations could lead to increased proliferation and diminished apoptosis of malignant T cells (see Fig. 4 for hypothetical model). Indeed, we show that several of these potentially biologically relevant genes show altered gene expression at RNA level (*TWIST, MXI1, MNT,* and *cMYC*) and protein level (*cMYC*). Nevertheless, to further substantiate the functional significance of the identified gene protein products in the pathogenesis of Sz, additional (functional) studies are clearly needed.

Most importantly, our data suggest that cMYC, TWIST, and STAT proteins provide promising novel therapeutic targets in the treatment of Sz. Several approaches to target cMYC are presently under investigation (47–49), and similarly, novel series of inhibitors of STAT proteins (e.g., cucurbitacins) are currently tested in clinical trials and might, if proven safe and effective, lead to new therapeutic approaches in Sz (50, 51). Because present treatment of Sz is largely unsatisfactory, additional studies to validate these novel therapeutic targets in larger numbers of patients are clearly warranted.

Acknowledgments

Received 11/28/2007; revised 1/9/2008; accepted 1/23/2008.

Grant support: The Netherlands Organisation for Health Research and Development grant 907-00-066 (M.H. Vermeer) and the EU-FP6 ENhanced LIGase Based Histochemical Techniques Project grant (U. Landegren).

The costs of publication of this article were defrayed in part by the payment of page charges. This article must therefore be hereby marked *advertisement* in accordance with 18 U.S.C. Section 1734 solely to indicate this fact.

We thank Dr. Y. Qin (Leiden University Medical Center, Leiden, the Netherlands) and Dr. T. Mitchell (King's College, London, United Kingdom) for their contribution to the quantitative real-time PCR experiments.

References

1. Willemze R, Jaffe ES, Burg G, et al. WHO-EORTC classification for cutaneous lymphomas. Blood 2005;105:3768–85.
2. Batista DA, Vonderheid EC, Hawkins A, et al. Multicolor fluorescence *in situ* hybridization (SKY) in mycosis fungoides and Sézary syndrome: search for recurrent chromosome abnormalities. Genes Chromosomes Cancer 2006;45:383–91.
3. Mao X, Lillington DM, Czepulkowski B, Russell-Jones R, Young BD, Whittaker S. Molecular cytogenetic characterization of Sézary syndrome. Genes Chromosomes Cancer 2003;36:250–60.
4. Karenko L, Kahkonen M, Hyytinen ER, Lindlof M, Ranki A. Notable losses at specific regions of chromosomes 10q and 13q in the Sézary syndrome detected by comparative genomic hybridization. J Invest Dermatol 1999;112:392–5.
5. Mao X, Lillington D, Scarisbrick JJ, et al. Molecular cytogenetic analysis of cutaneous T-cell lymphomas: identification of common genetic alterations in Sézary syndrome and mycosis fungoides. Br J Dermatol 2002;147:464–75.
6. Scarisbrick JJ, Woolford AJ, Russell-Jones R, Whittaker SJ. Allelotyping in mycosis fungoides and Sézary syndrome: common regions of allelic loss identified on 9p, 10q, and 17p. J Invest Dermatol 2001;117:663–70.
7. Mao X, Orchard G, Vonderheid EC, et al. Heterogeneous abnormalities of CCND1 and RB1 in primary cutaneous T-cell lymphomas suggesting impaired cell cycle control in disease pathogenesis. J Invest Dermatol 2006;126:1388–95.
8. Mao X, Orchard G, Lillington DM, Russell-Jones R, Young BD, Whittaker SJ. Amplification and overexpression of JUNB is associated with primary cutaneous T-cell lymphomas. Blood 2003;101:1513–9.
9. Karenko L, Hahtola S, Paivinen S, et al. Primary cutaneous T-cell lymphomas show a deletion or translocation affecting NAV3, the human UNC-53 homologue. Cancer Res 2005;65:8101–10.
10. Kari L, Loboda A, Nebozhyn M, et al. Classification and prediction of survival in patients with the leukemic phase of cutaneous T cell lymphoma. J Exp Med 2003;197:1477–88.
11. van Doorn R, Dijkman R, Vermeer MH, et al. Aberrant expression of the tyrosine kinase receptor EphA4 and the transcription factor twist in Sézary syndrome identified by gene expression analysis. Cancer Res 2004;64:5578–86.
12. Smit MJ, Verdijk P, van der Raaij-Helmer EM, et al. CXCR3-mediated chemotaxis of human T cells is regulated by a Gi- and phospholipase C-dependent pathway and not via activation of MEK/p44/p42 MAPK nor Akt/PI-3 kinase. Blood 2003;102:1959–65.
13. Knijnenburg J, Szuhai K, Giltay J, et al. Insights from genomic microarrays into structural chromosome rearrangements. Am J Med Genet 2005;132:36–40.
14. Dijkman R, Tensen CP, Jordanova ES, et al. Array-based comparative genomic hybridization analysis reveals recurrent chromosomal alterations and prognostic parameters in primary cutaneous large B-cell lymphoma. J Clin Oncol 2006;24:296–305.
15. La Rosa P, Viara E, Hupe P, et al. VAMP: visualization and analysis of array-CGH, transcriptome and other molecular profiles. Bioinformatics 2006;22:2066–73.
16. Hoefnagel JJ, Dijkman R, Basso K, et al. Distinct types of primary cutaneous large B-cell lymphoma identified by gene expression profiling. Blood 2005;105:3671–8.
17. Szuhai K, Tanke HJ. COBRA: combined binary ratio labeling of nucleic-acid probes for multi-color fluorescence *in situ* hybridization karyotyping. Nat Protoc 2006;1:264–75.
18. Szuhai K, IJszenga M, Tanke HJ, et al. Detection and molecular cytogenetic characterization of a novel ring chromosome in a histological variant of Ewing sarcoma. Cancer Genet Cytogenet 2007;172:12–22.
19. Söderberg O, Gullberg M, Jarvius M, et al. Direct observation of individual endogenous protein complexes *in situ* by proximity ligation. Nat Methods 2006;3:995–1000.
20. Jarvius M, Paulsson J, Weibrecht I, et al. *In situ* detection of phosphorylated platelet-derived growth factor receptor β using a generalized proximity ligation method. Mol Cell Proteomics 2007;6:1500–9.
21. Rouveirol C, Stransky N, Hupe P, et al. Computation of recurrent minimal genomic alterations from array-CGH data. Bioinformatics 2006;22:849–56.
22. Egle A, Harris AW, Bouillet P, Cory S. Bim is a suppressor of Myc-induced mouse B cell leukemia. Proc Natl Acad Sci U S A 2004;101:6164–9.
23. Hemann MT, Bric A, Teruya-Feldstein J, et al. Evasion of the p53 tumor surveillance network by tumor-derived MYC mutants. Nature 2005;436:807–11.
24. Valsesia-Wittmann S, Magdeleine M, Dupasquier S, et al. Oncogenic cooperation between H-Twist and N-Myc overrides failsafe programs in cancer cells. Cancer Cell 2004;6:625–30.
25. Puisieux A, Valsesia-Wittmann S, Ansieau S. A twist for survival and cancer progression. Br J Cancer 2006;94:13–7.
26. Krammer PH. CD95's deadly mission in the immune system. Nature 2000;407:789–95.
27. Kovanen PE, Rosenwald A, Fu J, et al. Analysis of γ c-family cytokine target genes. Identification of dual-specificity phosphatase 5 (DUSP5) as a regulator of mitogen-activated protein kinase activity in interleukin-2 signaling. J Biol Chem 2003;278:5205–13.
28. Wales MM, Biel MA, el Deiry W, et al. p53 activates expression of HIC-1, a new candidate tumor suppressor gene on 17p13.3. Nat Med 1995;1:570–7.
29. Issa JP, Zehnbauer BA, Kaufmann SH, Biel MA, Baylin SB. HIC1 hypermethylation is a late event in hematopoietic neoplasms. Cancer Res 1997;57:1678–81.
30. Wain EM, Mitchell TJ, Russell-Jones R, Whittaker SJ. Fine mapping of chromosome 10q deletions in mycosis fungoides and Sezary syndrome: identification of two discrete regions of deletion at 10q23.33-24.1 and 10q24.33-25.1. Genes Chromosomes Cancer 2005;42:184–92.
31. Dalla-Favera R, Bregni M, Erikson J, Patterson D, Gallo RC, Croce CM. Human c-myc onc gene is located on the region of chromosome 8 that is translocated in Burkitt lymphoma cells. Proc Natl Acad Sci U S A 1982;79:7824–7.
32. Weng AP, Millholland JM, Yashiro-Ohtani Y, et al. c-Myc is an important direct target of Notch1 in T-cell acute lymphoblastic leukemia/lymphoma. Genes Dev 2006;20:2096–109.
33. Henriksson M, Luscher B. Proteins of the Myc network: essential regulators of cell growth and differentiation. Adv Cancer Res 1996;68:109–82.
34. Soucek L, Evan G. Myc—is this the oncogene from hell? Cancer Cell 2002;1:406–8.
35. Nilsson JA, Maclean KH, Keller UB, Pendeville H, Baudino TA, Cleveland JL. Mnt loss triggers Myc transcription targets, proliferation, apoptosis, and transformation. Mol Cell Biol 2004;24:1560–9.
36. Dezfouli S, Bakke A, Huang J, Wynshaw-Boris A, Hurlin PJ. Inflammatory disease and lymphomagenesis caused by deletion of the Myc antagonist Mnt in T cells. Mol Cell Biol 2006;26:2080–92.
37. Hurlin PJ, Zhou ZQ, Toyo-oka K, et al. Deletion of Mnt leads to disrupted cell cycle control and tumorigenesis. EMBO J 2003;22:4584–96.
38. Zhang Q, Nowak I, Vonderheid EC, et al.Activation of Jak/STAT proteins involved in signal transduction pathway mediated by receptor for interleukin 2 in malignant T lymphocytes derived from cutaneous anaplastic large T-cell lymphoma and Sézary syndrome. Proc Natl Acad Sci U S A 1996;93:9148–53.
39. Eriksen KW, Kaltoft K, Mikkelsen G, et al. Constitutive STAT3-activation in Sézary syndrome: tyrphostin AG490 inhibits STAT3-activation, interleukin-2 receptor expression and growth of leukemic Sézary cells. Leukemia 2001;15:787–93.
40. Mitchell TJ, Whittaker SJ, John S. Deregulated expression of COOH-terminally truncated Stat5 and

loss of IL2-inducible Stat5-dependent gene expression in Sézary Syndrome. Cancer Res 2003;63:9048–54.
41. Qin JZ, Kamarashev J, Zhang CL, Dummer R, Burg G, Dobbeling U. Constitutive and interleukin-7- and interleukin-15-stimulated DNA binding of STAT and novel factors in cutaneous T cells lymphoma cells. J Invest Dermatol 2001;117:583–9.
42. Williams TM, Montoya G, Wu Y, Eddy RL, Byers MG, Shows TB. The TCF8 gene encoding a zinc finger protein (Nil-2-a) resides on human chromosome 10p11.2. Genomics 1992;14:194–6.
43. Yamanaka K, Clark R, Rich B, et al. Skin-derived interleukin-7 contributes to the proliferation of lymphocytes in cutaneous T-cell lymphoma. Blood 2006;107:2440–5.
44. Foss FM, Koc Y, Stetler-Stevenson MA, et al. Costimulation of cutaneous T-cell lymphoma cells by interleukin-7 and interleukin-2: potential autocrine or paracrine effectors in the Sézary syndrome. J Clin Oncol 1994;12:326–35.
45. Chen W, Cooper TK, Zahnow CA, et al. Epigenetic and genetic loss of Hic1 function accentuates the role of p53 in tumorigenesis. Cancer Cell 2004;6:387–98.
46. Wang Y, Putnam CD, Kane MF, et al. Mutation in Rpa1 results in defective DNA double-strand break repair, chromosomal instability and cancer in mice. Nat Genet 2005;37:750–5.
47. Oster SK, Ho CS, Soucie EL, Penn LZ. The myc oncogene: MarvelouslY Complex. Adv Cancer Res 2002;84:81–154.
48. D'Agnano I, Valentini A, Gatti G, Chersi A, Felsani A. Oligopeptides impairing the Myc-Max heterodimerization inhibit lung cancer cell proliferation by reducing Myc transcriptional activity. J Cell Physiol 2007;210:72–80.
49. Ponzielli R, Katz S, Barsyte-Lovejoy D, Penn LZ. Cancer therapeutics: targeting the dark side of Myc. Eur J Cancer 2005;41:2485–501.
50. Deng J, Grande F, Neamati N. Small molecule inhibitors of Stat3 signaling pathway. Curr Cancer Drug Targets 2007;7:91–107.
51. Haura EB, Turkson J, Jove R. Mechanisms of disease: insights into the emerging role of signal transducers and activators of transcription in cancer. Nat Clin Pract Oncol 2005;2:315–24.

Novel and Highly Recurrent Chromosomal Alterations in Sézary Syndrome

Maarten H. Vermeer, Remco van Doorn, Remco Dijkman, et al.

Cancer Res 2008;68:2689-2698.